The use of continuous high-frequency strain gauge measurements for the assessment of the role of ballast in stress reduction on steel railway bridge decks

W De Corte and Ph Van Bogaert

Although orthotropic plated decks are most frequently used for road bridges, some examples of the use of this type of decking for railway bridges exist. In these cases, the deck will be subject to higher loads as compared to road bridges, yet a number of mechanisms will lead to a better structural performance and use of the structural capacity of the deck, especially concerning fatigue. This latter phenomenon limits the design possibilities quite largely for road bridges, certainly for the deckplate. For railway bridges, a more favourable situation is created which is mostly overlooked. This situation is created by the threefold action of the stone ballast layer. The effectiveness of this action can most efficiently be tested by continuous strain gauge measurements on an in-service bridge. This procedure does not disrupt the railway traffic, and allows the effects to be measured for various axle configurations at different speeds. However, it requires the use of continuous and high-speed measurements as the measured strains change very fast. In addition, the measurements have to be taken very close to high-voltage electrical fields which disturb the small electrical signals in the sensor wiring. This article describes in detail the test set-up and the results from such tests carried out on two railway bridges in Belgium. In addition, the experimental results are linked to finite element calculations. This procedure permits not only a confirmation of the validity of the measured values and the calculation model, but also allows the calculations to be fine tuned.

Introduction

During recent years, a number of large steel bridges have been built for a high-speed railway line in Belgium. Due to vertical clearance and maximum vertical slope restrictions, the structural depth of these bridges has to be the smallest possible. For this reason, an orthotropic plated deck[1][2] has been chosen in several locations. This type of steel deck, combined with an arch as the main load carrying system, results in a low structural depth. Figure 1 displays two adjacent tied arch railway bridges with orthotropic decks. However, the slender bridge deck may suffer from heavy fatigue strength limitations, resulting from the many welded connections. Indeed, as the orthotropic deck consists of a series of longitudinal and transverse stiffeners welded to the lower side of a thin steel plate (see Figure 2), a large amount of welding is necessary.

One of the sensitive locations is the stiffener to deckplate connection. This joint is welded from one side only and has a low

W De Corte is Assistant Professor at Ghent University, Department of Civil Engineering, Technologiepark 904, 9052 Ghent, Belgium. Tel : +32 9 264 54 90; E-mail: Wouter.DeCorte@UGent.be

Ph Van Bogaert is a Professor at Ghent University, Department of Civil Engineering, Technologiepark 904, 9052 Ghent, Belgium. Tel : +32 9 264 54 90; E-mail: Philippe.VanBogaert@UGent.be

Figure 1. Tied arch bridges with orthotropic plated deck at Halle (Belgium)

fatigue resistance for transverse bending[3]. This bending can be substantial when a concentrated wheel load acts directly above the connection. Particularly for road bridges, the connection has led to cases of premature fatigue damage in various countries in Europe as well as in Japan. However, for railway bridges no cases of damage at this location have been reported. Indeed, as will be confirmed in this paper, the load dispersal through rails, sleepers and ballast, and due to the structural stiffness of the ballast layer itself, largely reduces the transverse bending at the stiffener to deckplate joint. In fact, the loads are almost entirely diverted to the

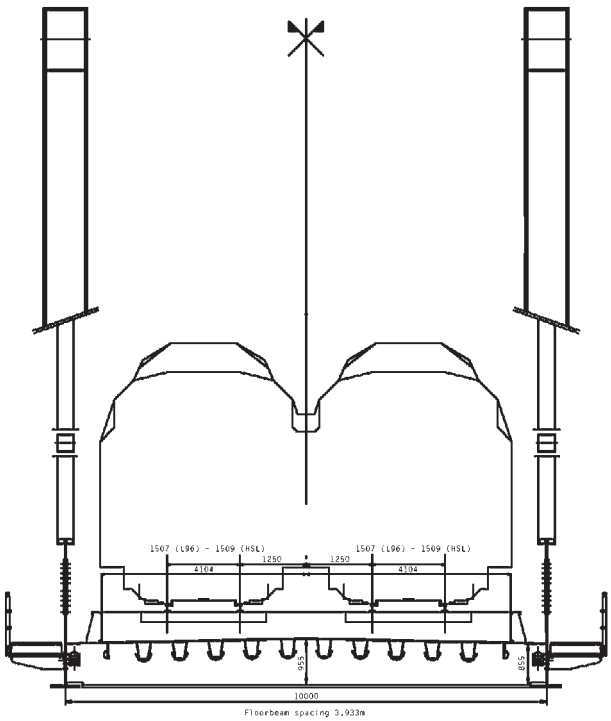

Figure 2. Cross-section of tied arch bridges with orthotropic deck at Halle (Belgium)

stiffener's vertical webs, rendering the transverse bending virtually to zero. This phenomenon has been overlooked in the past, partly due to the absence of damage and partly due to the complexity of the phenomenon. Indeed, the reduction can only be assessed accurately with continuous measurement equipment in combination with detailed finite element analysis. The stress reduction is not adequately addressed in the Eurocode normative documents[4][5], leading to larger then necessary minimum plate thicknesses.

Non-destructive measurements

General situation

The two bridges selected for the measurements are located in Halle, south of Brussels (Belgium), and cross a canal at a skew angle (see Figure 1). The first bridge is part of the Brussels to Paris high-speed railway link, whereas the other bridge carries national and freight traffic only. Both bridges are 115 m span tied arch with an orthotropic deck. The deck is made up of a 15 mm deckplate, longitudinally stiffened by 10 trapezoidal longitudinal stiffeners, spaced 750 mm apart, passing continuously through 1 m-high transverse floorbeams, spaced 4 m apart. The total width of the deck carrying two tracks is 10 m between the main beams. The UIC 60 (60 kg/m) rails are supported by monoblock prestressed concrete sleepers, and the ballast layer consists of 400 mm compacted crushed stone 40/60.

Basic test set-up

Short-based resistive strain gauges are chosen to assess the stresses in the deckplate in the vicinity of the stiffener to deckplate connection. They can provide accurate results in areas with large stress gradients remaining relatively easy to install. For this application they cannot be replaced by any other type of sensor, including optical sensors, in view of the required accuracy in positioning of the sensor, right next to the connection. Strain gauges are also easy to protect from the surrounding environment, especially moisture. The gauges are connected to a System 6000 Stress Analysis Data System (see Figure 3). This multifunctional acquisition system allows simultaneous registration of up to 20 channels, and can register up to 200,000 samples per second.

For this application, the unit is filled with 20 strain gauge signal acquisition cards. These cards feature a quarter of half bridge completion for 120, 300 and 1000 Ω strain gauges. In addition, selectable digital filtering is available, and the input voltage is programmable between 0.5 V and 10 V. The maximum sample frequency is limited to 10,000 samples per second per channel. However, due to the proximity of high-voltage electrical fields caused by the 15 kV high-speed line power feed, the maximum measurement frequency was limited to 200 samples per second, despite the electrical insulation of the connecting wires. Above these sample rates, the signal noise rapidly renders the results useless.

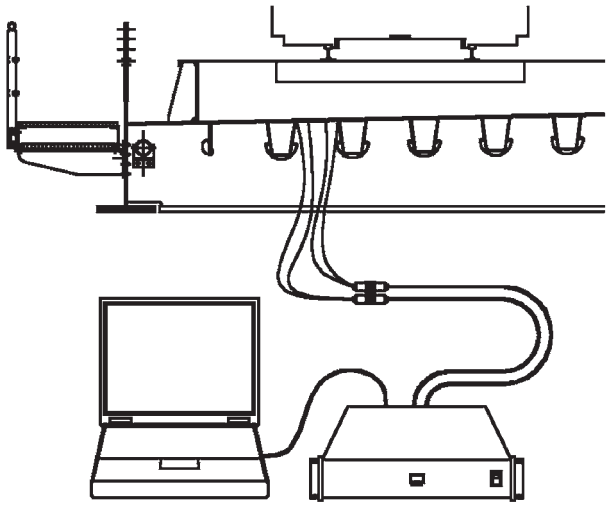

Figure 3. Test set-up

Additional test set-up

In order to link the gauge signals to the position of the axle loads responsible for the signal, two similar devices are used employing different electromagnetic sources. Both applications are based on the principle of beam disruption. An emitted light beam is blocked by the passing wheel, initiating a relay circuit. This circuit shunts a 120 Ω resistor with a 1 kΩ resistor. The acquisition device recognises this circuit as a strain gauge generating either a very low (not shunted) or a very high (shunted) fictive strain value. As both the effective strain gauges and the positioning circuit use an identical time base, any strain result can directly be linked to a specific position of the train on the bridge.

In the first device, the light beam is generated by a simple battery-powered laser pointer (1 mm beam diameter), aimed at a photo-voltaic cell (see Figure 4). The current generated by the beam is electronically amplified and keeps the relay circuit in the open position. During the crossing of the axle, the laser beam is blocked. The relay circuit closes and shunts the original resistor with the 1 kΩ resistor. In the second device, the laser pointer is replaced by an infrared emitter (see Figure 5) and, apart from this, both devices are identical. The IR emitter intrinsically has a wide beam, whereas the laser beam is practically one-dimensional. Consequently the signal

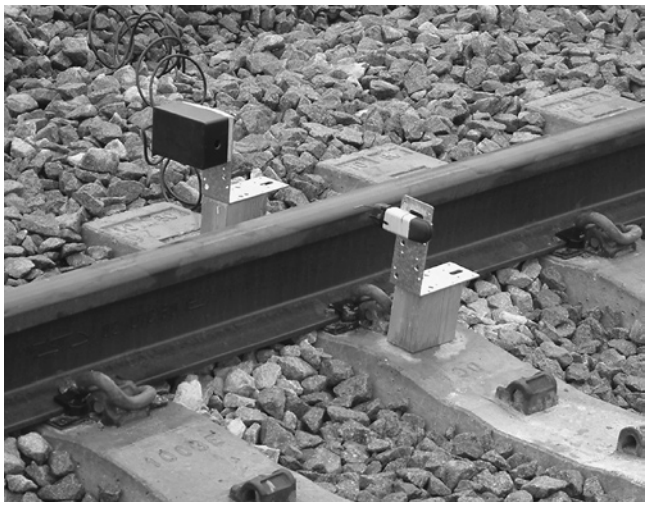

Figure 4. Laser-based positioning system

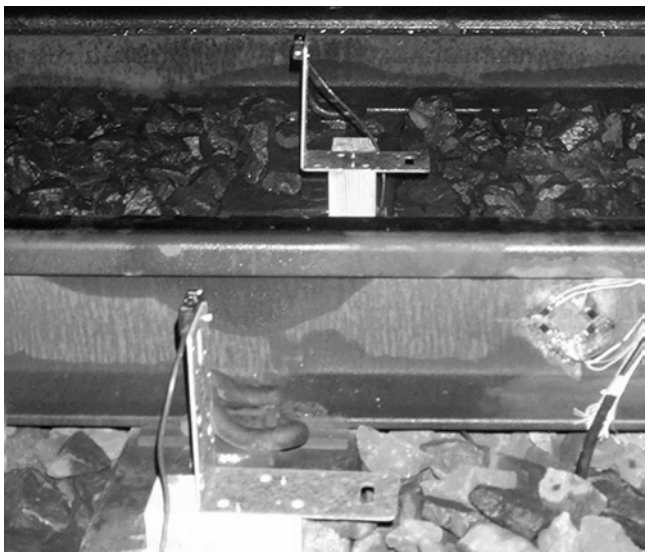

Figure 5. IR-based positioning system

change between the blocked and non-blocked signal occurs more gradually. The impact of this gradual change is, however, limited. On the other hand, where the positioning of the photo-voltaic cell needs to be done carefully for the laser beam application, this can be done very easily for the infrared device, in view of the difference in beam dimensions. In addition, the infrared device is less susceptible to vibrations, possibly causing beam misalignments.

Strain gauges and wiring

Criteria determining the choice of dimensions and configurations of strain gauges are the stress field gradient in the vicinity of the measurement location, the direction of the local principal strains and stresses and the ease of use during the application. The combination of these requirements results in a choice for a grid length of 3.18 mm, bearing in mind that the strain gauges have to be installed on the lower side of an in-service bridge deck. For this application, one single-grid strain gauge has been selected based on preliminary tests, indicating that the dominant stress field is one dimensional (transverse) only. Although measuring in only one direction reduces the effective accuracy of the measurements, it clearly increases the number of locations that can be measured simultaneously. Therefore, it was chosen in order to measure the strain at a larger number of points, but with slightly less accuracy.

The strain gauge application is carried out in a number of consecutive steps in accordance to the manufacturers' guidelines[6]. Essentially, it encompasses the mechanical removal of paint layers and rolling skin, a surface roughness treatment, surface degreasing and conditioning, and gauge adhesion. After wire soldering, the gauges are protected with an acid-free silicon layer.

All connecting wires are Defence Standard 61-12 Screened. These cables bundle 3 to 36 individual wires of 0.22 mm², and are protected from external electromagnetic fields by a metal wire netting. Despite the use of these protected wires and internal analogue and digital signal filtering, the sample frequency of each individual gauge could not be increased above 200 samples per second.

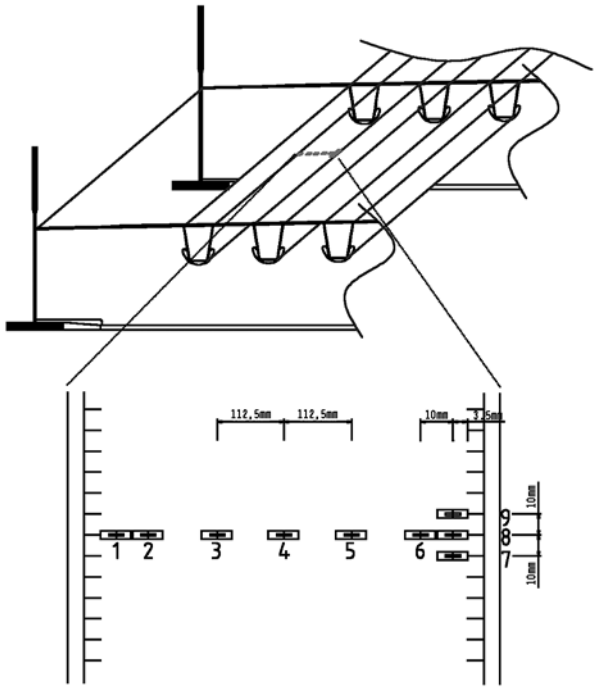

Figure 6. Position of gauges between 1st and 2nd stiffener

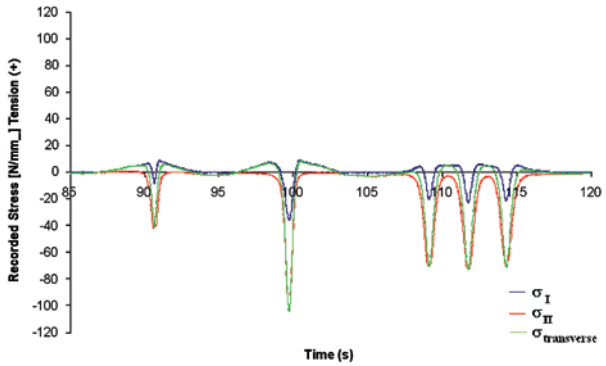

Figure 7. Stress results for a lorry crossing at Louvain

Results of strain gauge measurements

A group of nine strain gauges was positioned at the lower side of the 15 mm deckplate at different positions between the first and second stiffener, directly under the wheel, to measure the transverse plate bending (see Figure 6). All gauges are installed to measure transverse stresses only. Measurements with a heavy lorry on a similar bridge[7][8], before ballast and tracks were put in place, have revealed that high local transverse bending stresses in the plate do occur when a concentrated load is placed near the stiffener to deckplate connection. Figure 7 displays a recording of such a crossing, displaying transverse stress values for a gauge positioned directly adjacent to the connection, comparable to gauges 1 or 9. The transverse strain cycles reach values over 100 MPa, which would be unacceptable from a fatigue point of view, should it be a road bridge with a thin surfacing. During the tests on the bridges in Halle, the stress results for gauges 1 to 9 have been recorded for various high-speed trains and several passenger and freight trains.

As an example, Figures 8 and 9 give the results for gauges 1 and 4 for the crossing of a Thalys High-Speed Train (see Figure 8) and an electric locomotive (see Figure 9). In these Figures the x-axis represents the position of the first axle, as recorded by the laser (Thalys) or IR (locomotive) sensor *versus* the location of the strain gauge. In this way the results can easily be compared or related to finite element calculations, removing the effect of the vehicle

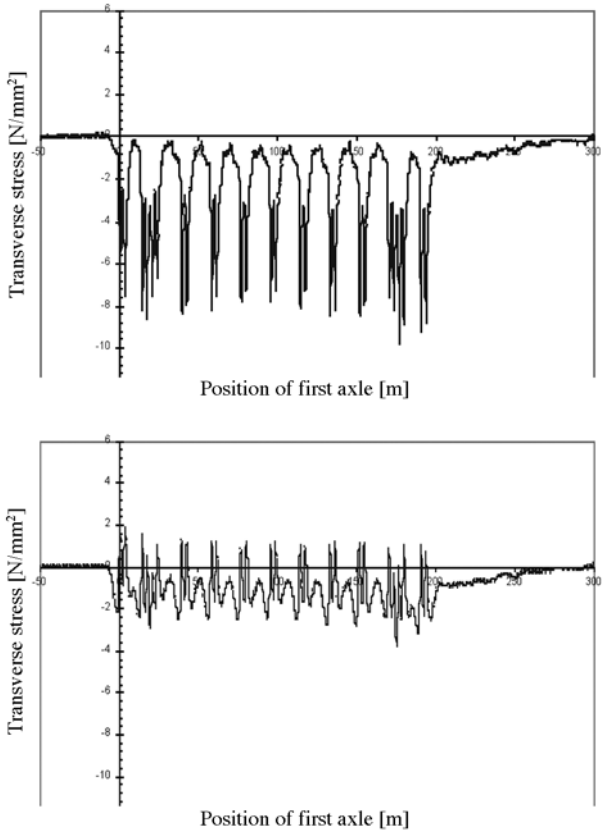

Figure 8. Recordings during Thalys crossing at Halle

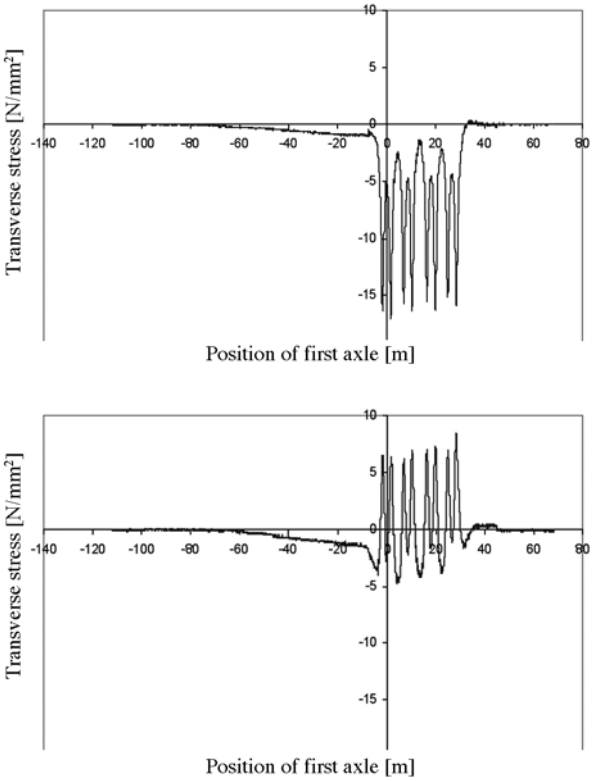

Figure 9. Recording during 2 locomotives crossing at Halle

speed. Travelling at over 160 km/h, the crossing of the high-speed train at the gauge location takes only five seconds, proving the need for the 200 Hz sample frequency. Remarkably, despite the high crossing speed, hardly any dynamic effect is present in the recorded signal, behaving as if the crossing were quasi-static. The fact that the signal does not immediately return to zero after the crossing can simply be attributed to co-operation of the orthotropic deck in the overall bridge action. As the location of the strain gauges is close to the support and the tracks directly above the gauges for the two bridges are in opposite direction, this effect is predominant after the crossing for the Thalys, and before the crossing for the locomotive.

Comparison of results on both bridges

Clearly, the results of both recordings cannot be compared directly as the axle configurations are substantially different. Using a back-calculating technique, the recordings are transformed to influences lines for individual axles, reduced to a 1 kN fictive axle load. The values for the Thalys have to be multiplied by 170 kN, and the values for the locomotive by 230 kN. Figure 10 produces these influence lines for the Thalys, and Figure 11 produces these influence lines for the locomotive. Here, the x-axis represents the position of the single axle *versus* the location of the strain gauges. The qualitative match between Figures 10 and 11 is obvious. Quantification is done for the maximum values of the influence lines at an abscissa value of 0, corresponding to an axle located directly above the gauge location, obviously generating the largest value. The result of this comparison is seen in Figure 12. Indeed, both transverse curves, generated by connecting the zero abscissa values from the influence lines from Figures 10 and 11, practically coincide. This proves not only the accuracy of the measurement, thanks to the adequate choice of strain gauges and measurement speed, but also indicates that the result is indeed independent of the crossing speed.

The remaining differences can be attributed to the tolerance on the effective orthotropic plate dimensions and plate thicknesses, to the tolerances on the effective positioning and alignment of the

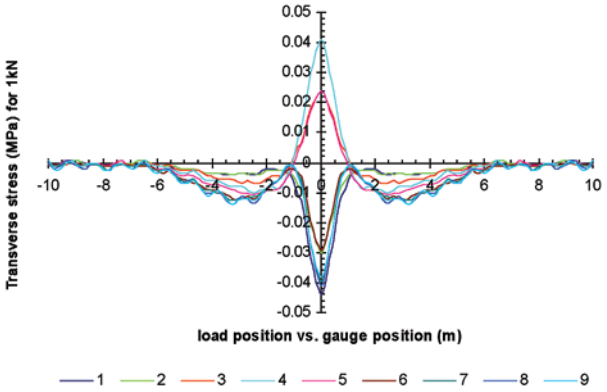

Figure 10. Back-calculated influence lines based on Thalys recordings

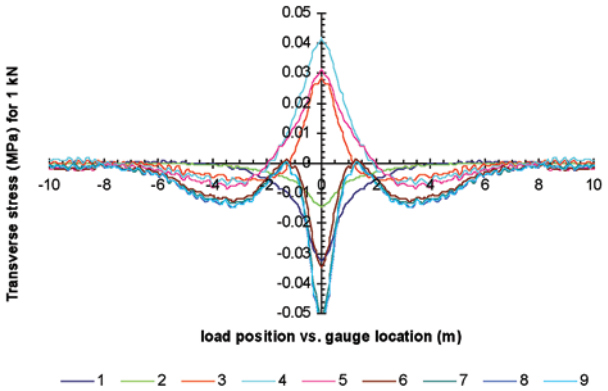

Figure 11. Back-calculated influence lines based on locomotive recordings

strain gauges, to the fact that the ballast layer is a discontinuous medium of which the characteristics may differ slightly from point to point, and to a small dynamic effect.

It should be noted that the maximum values for gauges 3, 4, and 5 differ only slightly. This implies that the transverse bending moment is almost constant between gauges 3 and 5. Knowing that a constant bending moment requires the applied load to be close to zero proves that the loading is certainly not uniformly distributed between gauges 1 and 9. It is concentrated near the stiffener to deckplate connection, because of the stiffness of the stiffener web.

Verification of obtained results with finite element analysis

The substantial reduction of transverse deckplate bending for ballasted rail systems originates from a threefold action in the ballast layer:

- The relatively low vertical stiffness of the ballast layer ensures that the local axle loads are carried by three adjacent sleepers; the load on the middle sleeper is reduced to a value of the order of 50% of its original value.
- Due to its own thickness, the ballast layer creates load spreading and the highly concentrated vertical pressure under the sleepers are spread over a larger surface.
- The stiffener webs create transversely stiff points for the deck plate. These stiffer supports introduce a distinct vaulted arch action in the ballast, by which the load is transferred to the stiffer supports relieving the deck plate areas between the stiffener webs. The ballast layer itself creates these arches, spanning from stiffener web to stiffener web. The vertical pressure generated by the sleepers is unevenly distributed through the ballast layer and acts more concentrated around these webs, reducing transverse bending moments and consequently the stresses at the fatigue sensitive location at the stiffener to deck plate joint.

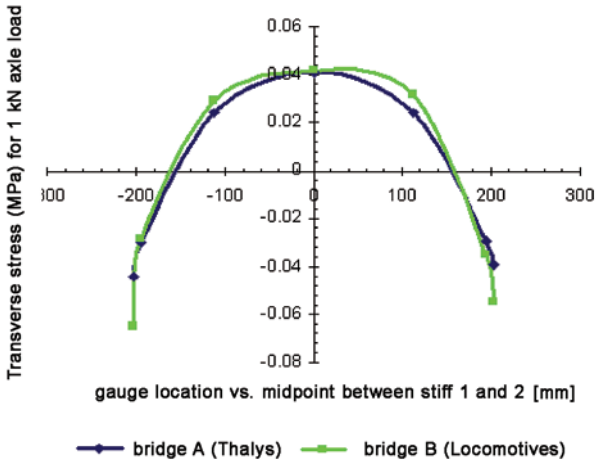

Figure 12. Maxima of back-calculated influence lines

This last action immediately relates to the observation made in the previous paragraph regarding the small difference between the recorded values of gauges 3, 4, and 5.

The presumed ballast actions and the experimental results are verified by a numerical analysis based on finite elements. For this reason, a 24 m-long section of the bridge deck was modelled, as well as the ballast layer, the concrete sleepers and the rails. Figure 13 gives a portion of this model, between two floorbeams. The details of this finite element model can be found in another publication[9]. Particularly important is the effective stiffness of the ballast material for which values of the Young's modulus between 150 and 300 MPa are found in the literature[10]. The layer, modelled as a continuum material, is connected vertically only to the deckplate. This implies that the ballast layer has to follow all vertical deck deflections, without any transfer of horizontal shear forces. Figure 14 gives calculated results of the transverse stresses for a 1 kN axle load at the lower side of the deckplate between the first and second stiffener, *ie* the location of the gauges, for different values of the ballast modulus ranging from 62.5 to 500 MPa. A comparison with the measured values indicates a stiffness value close to 200 MPa, which is perfectly acceptable. In time, the ballast stiffness may increase due to compaction caused by the railway traffic itself.

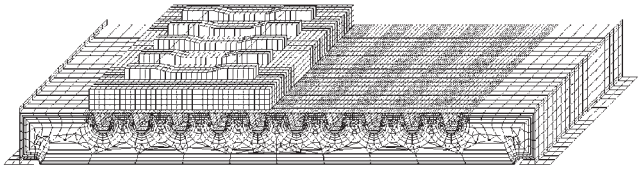

Figure 13. Finite element mesh

This agreement between the measured and calculated values confirms the validity of the calculation model, making it suitable for a parametric study into the effect of ballast thickness, stiffener shape, deckplate thickness, and stiffener spacing. Clearly, such a study is a logical follow-up to this experimental research.

Conclusions

This paper presents the application of high-speed strain gauge measurements on two in-service steel bridges. The application has enabled us to quantify the effect of the ballast layer stiffness on the transverse stresses in the deckplate, an effect previously overlooked. The reduction is very important for the guidelines

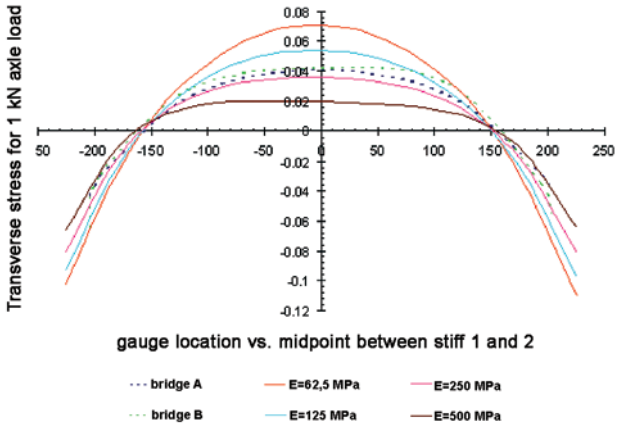

Figure 14. Comparison of FE-calculated and back-calculated maximum values

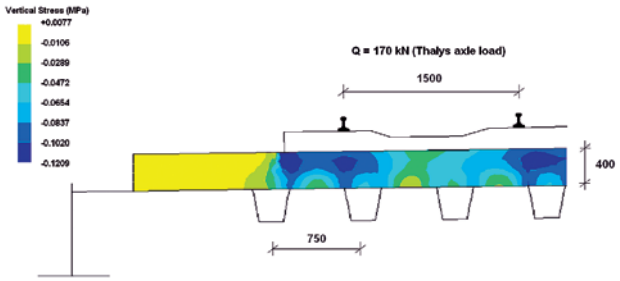

Figure 15. Transverse cut of FE result in ballast layer

given in the design codes for minimal plate thicknesses or stiffener spacing for the case of ballasted track railway bridges. Based on these observations the minimum required plate thickness can be reduced by at least 15%. Further mathematical study will provide the necessary guidelines for a range of configurations. However, such guidelines can be presumed to be validated by testing in view of the excellent results obtained.

References

1. R Wolchuk, 'Design manual for orthotropic steel plate deck bridges', AISC, 1963.
2. M S Troitsky, 'Orthotropic bridges – theory and design', The James F. Lincoln Arc Welding Foundation, Cleveland, 1967.
3. W De Corte, 'An improved detail category for trapezoidal stiffener to deckplate welds, based on full scale stress data and fatigue tests', Proc. of the 3rd International Conference on New Dimensions in Bridges and Flyovers, Kuala Lumpur, 2003.
4. European Committee for Standardization, 'Eurocode 1 Part 3: Traffic loads on bridges', Brussels, 1997.
5. European Committee for Standardization, 'Eurocode 3 Part 2: Design of steel structures – steel bridges', Brussels, 1997.
6. Measurements Group, Instruction Bulletin B-129, 'Surface preparation for strain gauge bonding'.
7. Ph Van Bogaert, 'Steel tied arch railway bridge, Louvain, Belgium', Structural Engineering International, Vol 1, pp 22-24, 2003.
8. W De Corte and Ph Van Bogaert, 'Assessment of fatigue strength of steel orthotropic plated bridge decks from continuous measured stress spectra', Proceedings IABSE Symposium, Antwerp, 2003.
9. W De Corte, 'Fatigue behaviour of steel orthotropic bridge decks subjected to traffic loads', PhD thesis, (in Dutch), 2005.
10. C Esveld, 'Modern railway track: second edition', 2001.